ISSN 0915-633X

NATIONAL INSTITUTE FOR FUSION SCIENCE

Separatrix Reconnection and Periodic Orbit Annihilation in the Harper Map

S. Saito, Y. Nomura, K. Hirose and Y.H. Ichikawa

(Received - Sep. 17, 1996)

NIFS-454 Oct. 1996

RESEARCH REPORT
NIFS Series

NAGOYA, JAPAN

Separatrix Reconnection and Periodic Orbit Annihilation in the Harper Map

[1] Satoshi Saitô, [2] Yasuyuki Nomura

[3] Keiichi Hirose and [3] Yoshi H. Ichikawa

[1] School of Engineerging, Nagoya University, Nagoya 464-01

[2] Fukui National College of Technology, Sabae 916

[3] College of Engineering, Chubu University, Kasugai 487

Abstract

Structure of the periodic accelerator orbits of the Harper map is investigated in detail from the view point of underlying scenario of chaos in the area preserving nontwist map. Since the twist function of the Harper map admits rigorous treatment for the entire range of phase variable, the results obtained in the present analysis describes generic novel phenomena, which are outside of the applicability of the Kolmogorov-Arnol'd-Moser theory.

Keywords

Harper map, non twist map, accelerator mode,

§1. Introduction

The recent advancement on studies of stochasticity in Hamiltonian systems with few degrees of freedom sheds new insight on interrelationship between statistical mechanics and dynamics. At the same time, the long time behaviour of the Hamiltonian systems has been key issues in high energy particle accelerator devices, magnetic confinement of plasma in fusion devices and wave heating of plasma. We can extend the list of fields to include astronomy. chemistry, fluid dynamics and condensed matter physics where the results of modern Hamiltonian dynamics have been successfully applied [1, 2]. Studies on the Hamiltonian dynamical system have been based on fundamental notions such as the Kolmogorov-Arnol'd-Moser (KAM in short) theorem and the Poincaré-Birkhoff theorem, which are proved to be valid if the unperturbed part of the Hamiltonian H_0 satisfies the nondegeneracy condition

$$\frac{\partial^2 H_0}{\partial I^2} \neq 0, \tag{1}$$

where I stands for action variable. In the discretized mapping description of Hamiltonian dynamics, the nondegeneracy condition (1) corresponds to the twist condition

$$\frac{\partial \theta_{n+1}}{\partial I_n} \neq 0, \tag{2}$$

where action-angle variables (I_n, θ_n) are evaluated at discrete time n. The twist condition implies the monotonic change of the rotation number $\omega = \lim_{n\to\infty} \theta_n/n$.

Observing that twist condition is a critical assumption in the proofs of the KAM theorem, del-Castillo-Negrete *et al.*[3] have carried out detailed analysis of the area preserving nontwist map. They have analyzed novel processes of the separatrix reconnection, periodic orbit collision and the transition to chaos in the standard nontwist map, which are outside of the applicability of the KAM theory.

As noticed by [3], however, the standard quadratic-nontwist map

$$y_{n+1} = y_n - b\sin(2\pi x_n) \tag{3}$$

$$x_{n+1} = x_n + a(1 - y_{n+1}^2) \tag{4}$$

is a polynomial local expansion about the point where the twist condition fails. Therefore, it is questionable whether phenomena associated with this map have generic validity. In

this regard, we notice that Van der Weele *et al.* [1] have constructed a model map for the standard scenario of the birth and reconnection process of periodic orbits in the nontwist map.

Aim of the present paper is to undertake detailed analysis of the Harper map, in which the phase advancement is determined by a sinusoidal twist function. The sinusoidal function admits alternative occurrence of the maximum and minimum, where the twist condition is violated. Thus, we can investigate global behaviour of the area preserving nontwist map, without any reservation for the polynomial local approximation. Furthermore, it is worth to notice that in a special choice of the parameters the Harper map is reduced to the $\hat{M}_4^4$ map discussed by Zaslavskii *et al.* [5] in connection with the stochastic web.

Summarizing the fundamental properties of the Harper map in Section 2, we proceed to analyze processes of the separatrix reconnection and the periodic orbit collision. In Section 3 and 4, changing of the system parameter, we investigate the phenomena taking place for the odd and the even periodic motions, respectively. For the odd periodic orbits, we observe that the higher order elliptic and hyperbolic orbits collide and annihilate each other, while the period-1 fundamental mode never annihilate. For the even periodic orbits, the period-2 step-1 accelerator orbits form the vortex pair, which exhibits robust structure against the change of the parameter. The period-4 and higher order even periodic orbits, however, after forming the vortex pair, annihilate eventually. In the last section, we summarize the results observed in the present analysis and discuss certain aspects of the stochastic web and anomalous diffusion phenomena.

§2. The Fundamental Properties of The Harper Map

We consider the Harper system, which describes the electron motion in the tight-binding lattice in the presence of magnetic field [6, 7, 8, 9, 10]. The Hamiltonian of this model has the form

$$H(q,p,t) = \frac{L}{4\pi^2}\cos 2\pi p + \frac{A}{4\pi^2}\cos 2\pi q \sum_{n=-\infty}^{\infty}\delta(t-n), \tag{5}$$

where q and p denote the dimensionless generalized position and momentum, respectively. A and L are the positive stochastic parameters.

The dynamics governed by the Hamiltonian (5) is described in terms of the mapping,

$$T: \begin{cases} p_{n+1} &= p_n + F(q_n) \\ & \qquad \text{(mod 1)} \\ q_{n+1} &= q_n + G(p_{n+1}) \end{cases} \tag{6}$$

with the definition of

$$F(q) = \frac{A}{2\pi} \sin 2\pi q \tag{7}$$

$$G(p) = -\frac{L}{2\pi} \sin 2\pi p. \tag{8}$$

We call this map the Harper map. Since the Jacobian of (6) is equal to unity, the Harper map (6) is the area-preserving. Since the functions $F(q)$ and $G(p)$ possess extrema, the Harper map is a nontwist map.

For small values of parameters A and L, there is a regular separatrix mesh on the phase plane. In general, when the value of A is different from L, the separatrix mesh is destroyed. In the case of $A > L$, there appear the rotational motion in the p direction, while in the case of $A < L$, there appear the rotational motion in the q direction. In the special case of $A = L$, the Harper map is reduced to the $\hat{M}_4^4$ map which has been investigated thoroughly by Zaslavskii *et al.*[5].

The Harper map has 4 fixed points such as $(q,p) = (0,0), (0,\frac{1}{2}), (\frac{1}{2},0)$ and $(\frac{1}{2},\frac{1}{2})$. The stability of these fixed points can be analyzed by means of the linear stability theory. Among the 4 fixed points, $(q,p) = (0,0)$ and $(1/2,1/2)$ become stable elliptic points under the condition $0 < AL < 4$. The nearby orbits encircle this elliptic point. The other two fixed points $(q,p) = (0,1/2), (1/2,0)$ turn to be always unstable. The nearby orbits are hyperbolic.

When the values of parameter A and L are increased, system shows global stochasticity. Even in this case, there exist the integrable orbits called momentum accelerator mode. Investigation of accelerator modes is necessary to understand the anomalous enhancement of momentum diffusion [11]. Accelerator mode of period-m step-n exists when the m iterations of map (6) satisfies

$$p_{i+m} = p_i + n \tag{9}$$

$$q_{i+m} = q_i. \tag{10}$$

The Harper map (6) admits the period-1 step-1 (fundamental) accelerator mode (q_0, p_0) when

$$F(q_0) = 1 \tag{11}$$

$$G(p_0) = m \tag{12}$$

holds for any integer m. Equation (11) tells us that period-1 fundamental accelerator mode exists for $A > 2\pi$. Period-2 step-s accelerator mode (q_0, p_0) is determined from the squared Harper map according to the following condition for any integer m.

$$F(q_0) + F(q_0 + G(p_0 + F(q_0))) = s \tag{13}$$

$$G(p_0 + F(q_0)) + G(p_0 + F(q_0) + F(q_0 + G(p_0 + F(q_0)))) = m, \tag{14}$$

which suggests that the period-2 step-1 accelerator mode exists for $A < 2\pi$. In the course of this study, we have identified various higher order accelerator modes by decreasing A from 2π, as shown in Table 1. The stable domain for A and L need to be analyzed individually for each mode. The contribution of the period-2 accelerator mode to the enhancement of momentum diffusion has been identified by Saitô *et al.* [11]. Structure of the period-2 step-1 island appeared in the vicinity of $A = 3.185$ has been analyzed by Hirose *et al.*[12].

Since the Harper map is a typical nontwist map, we proceed to analyze the process of the separatrix reconnection and periodic orbit annihilation in detail.

§3. Reconnection and Annihilation of Odd Periodic Orbit

In this section, we discuss the separatrix reconnection and annihilation of several odd periodic accelerator modes taking place in the region of $A > L$.

First, we investigate the period-1 step-1 accelerator mode appeared at $A = 6.37$. The phase plane at $L = 0.004$ is shown in Fig. 1. We confirm the period-1 islands appeared as a pair. The motion around the right island is counter direction with respect to the motion around the left island. The position of the left elliptic point is $(q_1, p_1) = (\frac{1}{2\pi}\sin^{-1}(\frac{2\pi}{A}), 0)$ and that of the right elliptic points is $(q_2, p_2) = (\frac{1}{2} - q_1, \pm\frac{1}{2})$. The right separatrix has

hyperbolic point at $(q,p) = (q_2, 0)$ and the left separatrix passes through hyperbolic points at $(q,p) = (q_1, \pm\frac{1}{2})$. Between these separatrices, there are band of curves separating the right and the left islands. We also plot the symmetry lines summarized in Appendix I. They intersect at the period-1 elliptic and hyperbolic points.

Increasing the parameter L to $L = 0.009$, we observe in Fig. 2 the separatrix reconnection takes place in the vicinity of this value of L. In order to determine the critical value of L at which separatrix reconnection of the period-1 step-1 mode occurs, we introduce the averaged Hamiltonian [14]. Since the motion on the separatrix is considered to be slow, we can approximate $p_{n+1} - p_n$ and $q_{n+1} - q_n$ to be dp and dq, respectively. Therefore, the Harper map (6) can be reduced to a following differential equation.

$$\frac{dp}{dq} = -\frac{A\sin 2\pi q - 2m\pi}{L\sin 2\pi p} \tag{15}$$

where m is set to be 1 for the step-1 accelerator orbit. Integrating (15), we obtain the averaged Hamiltonian $\bar{H}(q,p)$

$$\bar{H}(q,p) = \frac{L}{4\pi^2}\cos 2\pi p + \frac{A}{4\pi^2}\cos 2\pi q + q. \tag{16}$$

The separatrix reconnection occurs when the averaged Hamiltonian of the right and the left separatrices

$$\bar{H}_{\rm left}(q_1, \pm\frac{1}{2}) = \frac{L}{4\pi^2} + \frac{A}{4\pi^2}\cos 2\pi q_1 + q_1, \tag{17}$$

$$\bar{H}_{\rm right}(q_2, 0) = -\frac{L}{4\pi^2} - \frac{A}{4\pi^2}\cos 2\pi q_1 + \frac{1}{2} - q_1 \tag{18}$$

have the same value. Thus, we obtain the critical value L_c,

$$L_c = -\sqrt{A^2 - 4\pi^2} + \pi^2 - 2\pi\sin^{-1}(\frac{2\pi}{A}). \tag{19}$$

In Fig. 3, we show the phase portrait of averaged Hamiltonian (16) at $A = 6.37$ and $L_c = 0.009561$. Comparing Fig. 2 and Fig. 3, we can confirm that our estimation of L_c is appropriate.

After the reconnection, the relative positions of the right and the left island are topologically interchanged to the left and the right. This is illustrated in Fig. 4 at $L = 0.02$. We observe that the separatrices form two dimerized chains named after Van der Weele [4].

As L is increased, the system becomes stochastic. At $L = 0.3$, shown in Fig. 5, we observe the dominant two stochastic layers. Between them, we see the evidence of separatrix reconnection of the period-11 islands, which form two dimerized chains. Del-Castillo-Negrete *et al.* called this self similarity structure the nested topology, which is shown in Fig. 10 in [3]. Since the positions of the period-1 points are independent of the parameter L, symmetry lines continue to have intersections at the same position as L is varied. Therefore, this implies that the annihilation of period-1 accelerator mode never take place.

Next, we investigate the period-3 step-1 accelerator mode, which appears at $A = 2.3$. We show the phase plane at $L = 0.9$ in Fig. 6. Period-3 islands appear as pairs in staggered manner. As L is increased, focusing our attention to the pair of elliptic and hyperbolic point with $p = 0$, we observe that neighboring two intersections approach and becomes one point at which symmetry lines tangent each other. Here the period-3 island annihilates, as shown in Fig. 7. This process is nothing but a tangent bifurcation. The critical value of L at which tangent bifurcation occurs can be determined by the tangent condition of γ_0 and γ_3.

We carried out the analysis for all of the odd periodic islands listed in the Table 1. We confirm that the process of the reconnection and annihilation are the same as the period-3 case. Thus, we conjecture that annihilation of periodic points occurs for all of the odd periodic points other than period-1 fundamental accelerator mode.

§4. Reconnection and Annihilation of Even Periodic Orbit

In this section, we analyze the separatrix reconnection and annihilation of even periodic accelerator modes. For even periodic case, the aligned counter rotating islands merge and the vortex pairs are formed.

We first investigate the period-2 step-1 accelerator mode appeared at $A = 3.185$. Figure 8 illustrates the phase plane at $L = 0.3$. Symmetry lines determines the position of elliptic and hyperbolic points. The position of the left elliptic points are $(q_1, p_1) = (\frac{1}{2\pi}\sin^{-1}(\frac{\pi}{A}), 0)$ and $(q_1, \pm\frac{1}{2})$ and that of the right elliptic points are $(q_2, p_2) = (\frac{1}{2} - q_1, 0)$ and $(\frac{1}{2} - q_1, \pm\frac{1}{2})$.

Since the position of the elliptic points are independent of the parameter L, these points do not annihilate upon the change of L. The left and the right separatrices pass through the hyperbolic points which are given as the left and right intersections of symmetry lines γ_{-1} and γ_1. In contrast to the odd periodic case, neighboring intersections are the same type each other.

As L is increased, the neighboring hyperbolic points approach, while the elliptic points do not move. The reconnection occurs when the right and left separatrices coincide together. After the reconnection, the pair of the period-2 islands form the vortex pair. This is illustrated in Fig. 9 at $L = 0.4$. Symmetry lines γ_{-1} and γ_1, which intersect at the hyperbolic points before the reconnection, do not intersect at hyperbolic points after the reconnection. We notice, however, that the positions of all of the period-2 points can be determined from the existing conditions (13) and (14) for the period-2 accelerator mode. After the reduction discussed in Appendix II, the position of hyperbolic points after the reconnection is determined by the conditions of (13) and (14)

$$F(q) = \frac{1}{2} \tag{20}$$

$$2q - G(p) = \frac{1}{2}. \tag{21}$$

Howard *et al.* [15] call this condition the resonance lines. First, we can determine the critical value L_c at which the separatrix reconnection occurs basing on the equations (20) and (21). Since they tangent each other at $p = \frac{1}{4}$, we obtain L_c as

$$L_c = \pi - 2\sin^{-1}(\frac{\pi}{A}) \tag{22}$$

$$= 0.33057\cdots \quad \text{for} \quad A = 3.185. \tag{23}$$

The positions of hyperbolic points after the reconnection are

$$(q_{\rm h}, p_{\rm h}) = (q_1, \frac{1}{2\pi}\sin^{-1}\{\frac{2\pi}{L}(\frac{1}{4} - q_1)\}) \tag{24}$$

$$= (q_1, \frac{1}{2} - \frac{1}{2\pi}\sin^{-1}\{\frac{2\pi}{L}(\frac{1}{4} - q_1)\}). \tag{25}$$

This is illustrated in Fig. 9. Although $q_{\rm h}$ is independent of L, $p_{\rm h}$ depends on it. $p_{\rm h}$ tends to 0, as $L \to \infty$. It means that the hyperbolic points after the reconnection approach to the elliptic points but do not annihilate.

Next, we investigate the period-4 accelerator mode appeared at $A = 1.8$. Figure 10 illustrates the phase plane at $L = 1.1$. We can see four vortex pairs and symmetry lines intersect at the elliptic point of the vortex islands. In Fig. 11 at $L = 1.2$, we observe that these intersections disappear and the elliptic point annihilates.

For other even periodic cases listed in Table 1, the process of the reconnection and the annihilation are the same as the period-4. Thus, we may conclude that annihilation of elliptic points occurs for all of the even periodic points other than period-2.

§4. Concluding Discussions

We have examined process of the separatrix reconnection and the periodic orbits collisions, focusing our attention to the accelerator modes in the Harper map, which contains two nonlinear parameters A and L. In the studies of the stochastic diffusion in the momentum space, the constant A determines the depth of nonlinear modulation in the momentum space, while the constant L characterizes a size of twist in the phase. We may call the constant A, stochastic parameter and the constant L, the twist parameter, respectively.

We remind that a special case of $A = L$ stands for the symmetric nonlinear map to describe the stochastic web. Referring to this special choice of parameters, Shinbrot *et al.*[13] have discussed control of transport in a chaotic lattice.

The present work has attempted to examine structure of the various order of the accelerator modes of the Harper map from the view point of generic properties of the nontwist map. Since the period-1 step-1 (fundamental) accelerator mode do not depend on the twist parameter L, the mode persists after the separatrix reconnection. As for the period-2 step-1 accelerator mode, the elliptic points are independent of the twist parameter L, while the hyperbolic points approach each other in the q-direction and then scattered towards the p-direction. Upon the increase of the twist parameter, the system exhibits feature of chaos with the robust structure of pairs of the elliptic period-2 step-1 accelerator mode. This is the process of the formation of vortex in the nonlinear map.

With regards the higher order odd periodic accelerator modes, we have observed that the elliptic point and the hyperbolic point collide each other and annihilate. This is nothing but

the inverse process of the tangent bifurcation. On the contrary, for the even periodic accelerator modes, pairs of the elliptic points form the vortex pair in the phase plane. Eventually the vortex pair annihilates for all of the even periodic orbits other than period-2.

We anticipate that these detailed mechanisms of the separatrix reconnection, the vortex pair formation and the annihilation of the periodic orbits are responsible to determine the so called stickiness around the islands in the Hamiltonian system. In order to provide quantitative information on the notion of the stickiness, we need investigate interrelationship between mechanism of these elementary processes and probabilistic estimate of the stickiness.

Acknowledgement

We thank T. Kamimura for his valuable discussion. This work was supported by the Collaborating Program of the National Institute for Fusion Science (NIFS).

§Appendix I: Involutions and Symmetry Lines

In order to analyze the structure of the periodic points, it is useful to consider the symmetry of the system [16, 17, 18].

For the Harper map, both of the transformation function $G(p)$ is antisymmetric with respect to momentum inversion, $G(-p) = -G(p)$. Let us investigate the accelerator modes appeared for $A > L$. In this case, the Harper map (6) may be expressed as the product of two involutions

$$T = I_1 I_0 \tag{26}$$

with $I_1^2 = I_0^2 = 1$ as follows.

$$I_0 \ : \ \begin{cases} p' &= -p \\ q' &= x - G(p) \end{cases} \tag{27}$$

$$I_1 \ : \ \begin{cases} p' &= -p + F(q - G(p)) \\ q' &= q - G(p) - G(p - F(q - G(p))) \end{cases} \tag{28}$$

$$\tag{29}$$

When T is factorized, involution I_j is defined for all integers j by

$$I_j = T^j I_0 \tag{30}$$

with $I_j^2 = 1$. A symmetry line γ_j for any integer j is formed by the set of fixed points of I_j

$$\gamma_j : \{R | I_j \cdot R = R\} \tag{31}$$

Then the important properties are derived from the definition of symmetry lines. The intersection of the symmetry lines γ_j and γ_i is a periodic point of period $|j-i|$. Symmetry line γ_j is transformed to γ_{2n+j} by T^n.

$$\gamma_{2n+j} = T^n \gamma_j. \tag{32}$$

The following recurrence relations hold.

$$\gamma_j(R) = \gamma_{j-2}(T^{-1}R) \tag{33}$$

$$\gamma_j(R) = \gamma_{j+2}(TR) \tag{34}$$

Examples of symmetry lines are following.

$$\gamma_0 : 2p = m \tag{35}$$

$$\gamma_1 : 2p - F(q - G(p)) = m \tag{36}$$

$$\gamma_2 : 2p - 2F(q - G(p)) = m \tag{37}$$

$$\gamma_3 : 2p - 2F(q - G(p)) - F(q - G(p) - G(p - F(q - G(p)))) = m \tag{38}$$

$$\gamma_4 : 2p - 2F(q - G(p)) - 2F(q - G(p) - G(p - F(q - G(p)))) = m \tag{39}$$

$$\gamma_{-1} : 2p + F(q) = m \tag{40}$$

$$\gamma_{-2} : 2p + 2F(q) = m \tag{41}$$

$$\gamma_{-3} : 2p + 2F(q - G(p)) + F(q + G(p + F(q))) = m \tag{42}$$

$$\gamma_{-4} : 2p + 2F(q - G(p)) + 2F(q + G(p + F(q))) = m \tag{43}$$

§Appendix II: Period-2 Accelerator Modes

We can determine all the position of period-2 accelerator mode by the existing conditions (13) and (14) . Let us consider this condition more carefully. Since the functions $F(q)$ and

$G(p)$ are sinusoidal, substituting (13) into (14), we obtain

$$G(p + F(q)) + G(p) = m. \tag{44}$$

Substituting (44) back into (13), we obtain

$$F(q) + F(q - G(p)) = s. \tag{45}$$

Focusing our attention to the period-2 step-1 accelerator mode, $s = 1$ and $m = 0$. Using the sinusoidal relation, (44) is written as

$$\sin \pi(2p + F(q)) \cos \pi F(q) = 0. \tag{46}$$

There are two cases which satisfy (46).

$$2p + F(q) = n \tag{47}$$

$$F(q) = \frac{2n - 1}{2}. \tag{48}$$

First, we solve (45) and (47) and then solve (45) and (48) later. Substituting (47) into (44), we obtain

$$2p - F(q - G(p)) = n'. \tag{49}$$

Thus the solutions of (45) and (47) are the intersections of (47) and (49).

Next, we solve (45) and (48). In the case of $n = 1$,

$$F(q) = \frac{1}{2}. \tag{50}$$

Then from (45) we obtain

$$F(q - G(p)) = \frac{1}{2}. \tag{51}$$

From (50) and (51), we obtain

$$\sin \pi G(p) \cos \pi(2q - G(p)) = 0. \tag{52}$$

Thus, the solutions are the intersections of the following lines.

$$p = \frac{n}{2} \tag{53}$$

$$F(q) = \frac{1}{2} \tag{54}$$

and

$$F(q) = \frac{1}{2} \tag{20}$$

$$2q - G(p) = \frac{1}{2}. \tag{21}$$

Equations (47) and (49) are nothing but the symmetry lines γ_{-1} and γ_1, respectively. Intersections of (53) and (54) are elliptic points. We can determine the hyperbolic points after the reconnection by (20) and (21).

References

[1] R. S. MacKay and J. D. Meiss, eds., Hamiltonian Dynamical Systems, a reprint selection (Adam-Hilger, London, 1987).

[2] I. E. Reichl, The Transition to Chaos in Conservative Classical Systems (Springer-Verlag, New York, 1992).

[3] D. del-Castillo-Negrete, J. M. Greene and P. J. Morrison, Physica D (1995) 101-100.

[4] J. P. Van der Weele and T. P. Valkering, PHysica A **169** (1990) 42-72.

[5] G. M. Zaslavskiĭ, M. Yu. Zakharov, R. Z. Sagdeev, D. A. Usikov, and A. A. Chernikov, Sov. Phys. JETP **64** (1986), 294.

[6] P. G. Harper, Proc. R. Soc. London, A**68** (1955), 874.

[7] D. R. Hofstadter, Phys. Rev. B**14** (1976), 2239.

[8] P. Leboeuf, J. Kurchan, M. Feingold, and D. P. Arovas, Phys. Rev. Lett. **65** (1990), 3076.

[9] T. Geisel, R. Ketzmerick, and G. Petschel, Phys. Rev. Lett. **67** (1991), 3635.

[10] R. Lima and D. L. Shepelyansky, Phys. Rev. Lett. **67** (1991), 1377.

[11] S. Saitô, Y. Nomura, and Y. H. Ichikawa, *Prog. Theor. Phys.* **94,745**(1995).

[12] K. Hirose, S. Saitô and Y. H. Ichikawa, to appear in Plasma Phys. Report 22 (1996) No.9.

[13] T. Shinbrot. L. Bresler and J. M. Ottino, Physica D93 (1996) p191-209.

[14] J. E. Howard and S. M. Hohs, Phys. Rev. A vol29 (1984) 418-421.

[15] J. E. Howard and J. Humpherys, Nonmonotonic twist maps, Physica D 80 (1995) 256-276.

[16] J. M. Greene. J. Math. Phys. **9** (1968), 760.

[17] J. M. Greene, J. Math. Phys. **20** (1979), 1183.

[18] R. de Vogelaere, Contributions ot the Theory of Nonlinear Oscillations Vol IV., ed. S. Lefschetz (Princeton U.P., Princeton, New Jersey, 1958).

§Figure Captions

Fig. 1. Phase plane of the period-1 step-1 accelerator mode at $A = 6.37$ and $L = 0.001$ with the symmetry lines $\gamma_j (j = -2, -1, 0, 1, 2)$.

Fig. 2. Phase plane of the period-1 step-1 accelerator mode at $A = 6.37$ and $L = 0.009$. Separatrix reconnection occurs in the vicinity of these parameter values.

Fig. 3. Phase plane of averaged Hamiltonian (16) at $A = 6.37$ and $L = L_c = 0.009561$.

Fig. 4. Phase plane of the period-1 step-1 accelerator mode at $A = 6.37$ and $L = 0.02$.

Fig. 5. Phase plane of the period-1 step-1 accelerator mode at $A = 6.37$ and $L = 0.3$. Between the two stochastic layers, two dimerized chains of the period-11 islands indicate the evidence of the separatrix reconnection.

Fig. 6. Phase plane of the period-3 step-1 accelerator mode at $A = 2.3$ and $L = 0.9$. Period-3 islands appear as pairs in staggered manner. The position of the hyperbolic points are identified with the intersection of the symmetry lines.

Fig. 7. Phase plane of the period-3 step-1 accelerator mode at $A = 2.3$ and $L = 1.3$. After symmetry lines tangent each other, the period-3 orbits annihilate.

Fig. 8. Phase plane of the period-2 step-1 accelerator mode at $A = 3.185$ and $L = 0.3$ with the symmetry lines $\gamma_j (j = -2, -1, 0, 1, 2)$. The counter rotating islands appear in the aligned manner.

Fig. 9. Phase plane of the period-2 step-1 accelerator mode at $A = 3.185$ and $L = 0.4$. The hyperbolic points approach in the q direction and scattered toward the p direction. Period-2 islands form the vortex pairs. Symmetry lines of γ_1 and γ_{-1} never intersect at the hyperbolic points after the reconnection. Intersections of lines of Eq. (20) and (21) determine the hyperbolic points after the reconnection. The line (21) passes through just between the vortex islands.

Fig. 10. Phase plane of the period-4 step-1 accelerator mode at $A = 1.8$ and $L = 1.1$ with the symmetry lines $\gamma_j (j = -4, -3, -2, -1, 0, 1, 2, 3, 4)$. There appear the 4 vortex pairs. Since this is after the reconnection, there is no intersection of symmetry lines. at the hyperbolic points.

Fig. 11. Phase plane of the period-4 step-1 accelerator mode at $A = 1.8$ and $L = 1.2$. After the symmetry lines of γ_{-1} and γ_3 tangent each other, the period-4 elliptic points annihilate.

§Table Caption

Table I. The list of the accelerator modes of the Harper map.

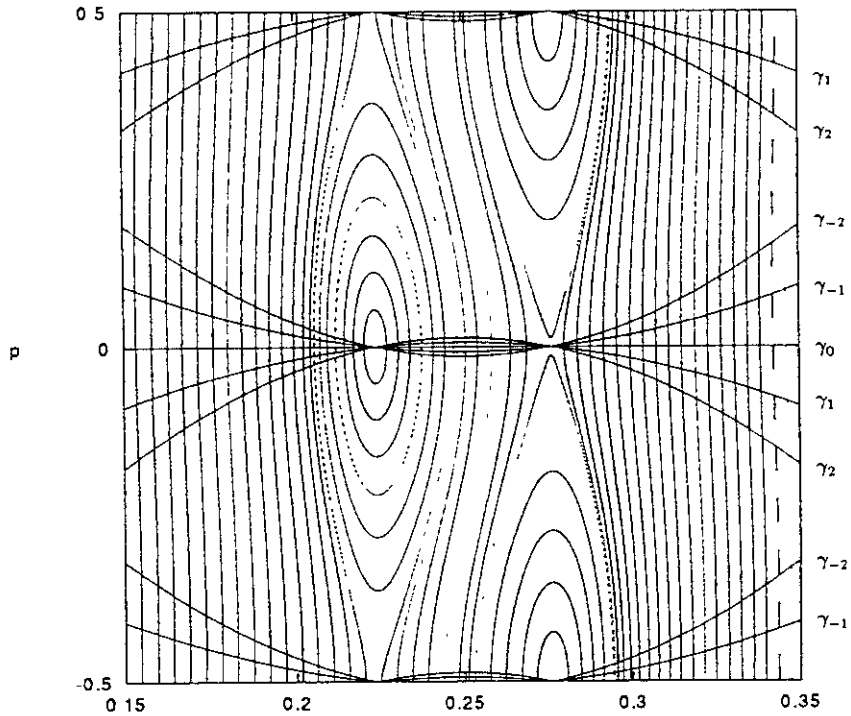
0 5
p
0
-0.5
0 15
0.2
0.25
0.3
0.35
q
γ_1
γ_2
γ_{-2}
γ_{-1}
γ_0
γ_1
γ_2
γ_{-2}
γ_{-1}

Fig. 1

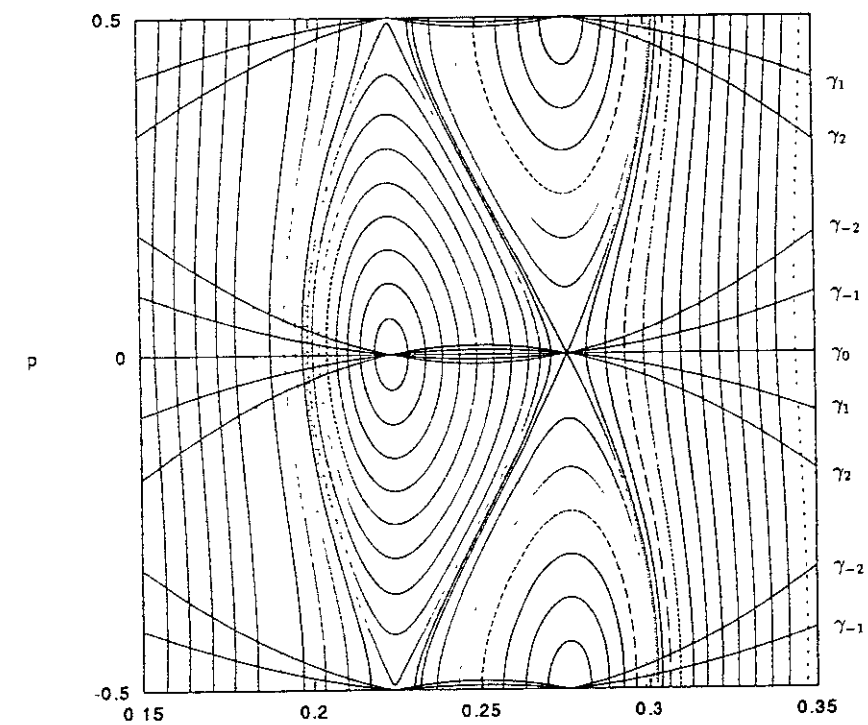
0.5
p
0
-0.5
0 15
0.2
0.25
0.3
0.35
q
γ_1
γ_2
γ_{-2}
γ_{-1}
γ_0
γ_1
γ_2
γ_{-2}
γ_{-1}

Fig. 2

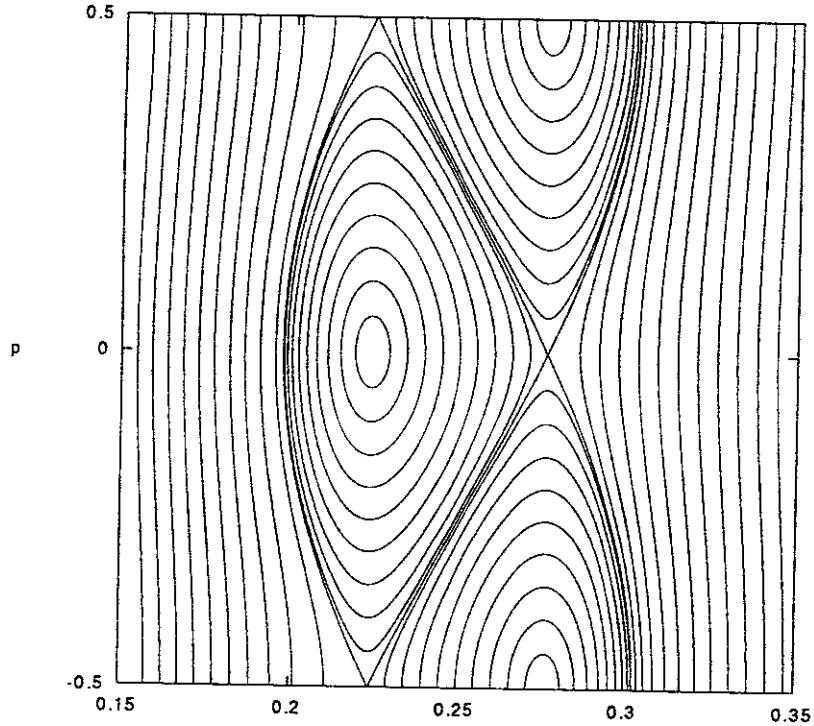
0.5
p
0
-0.5
0.15
0.2
0.25
0.3
0.35
q

Fig 3

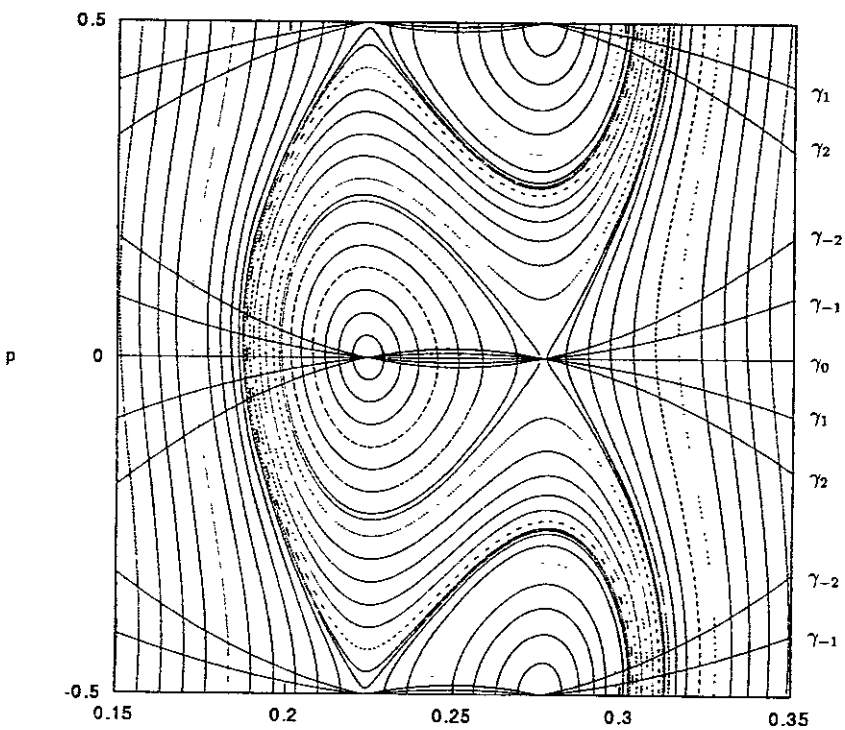
0.5
p
0
-0.5
0.15
0.2
0.25
0.3
0.35
q
γ_1
γ_2
γ_{-2}
γ_{-1}
γ_0
γ_1
γ_2
γ_{-2}
γ_{-1}

Fig. 4

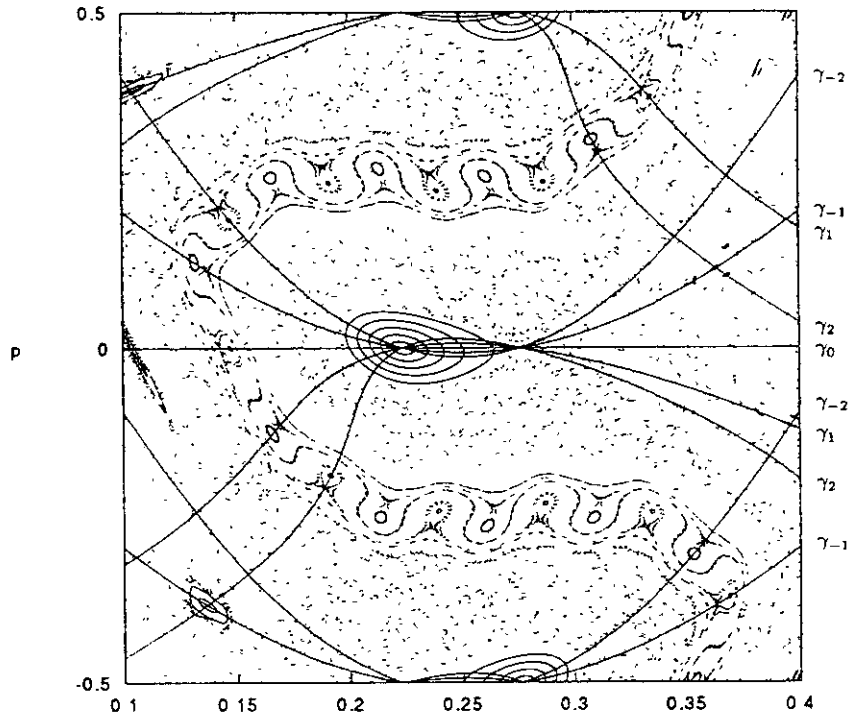
0.5
0
-0.5
p
0 1
0 15
0.2
0.25
0.3
0.35
0 4
q
γ−2
γ−1
γ1
γ2
γ0
γ−2
γ1
γ2
γ−1

Fig 5

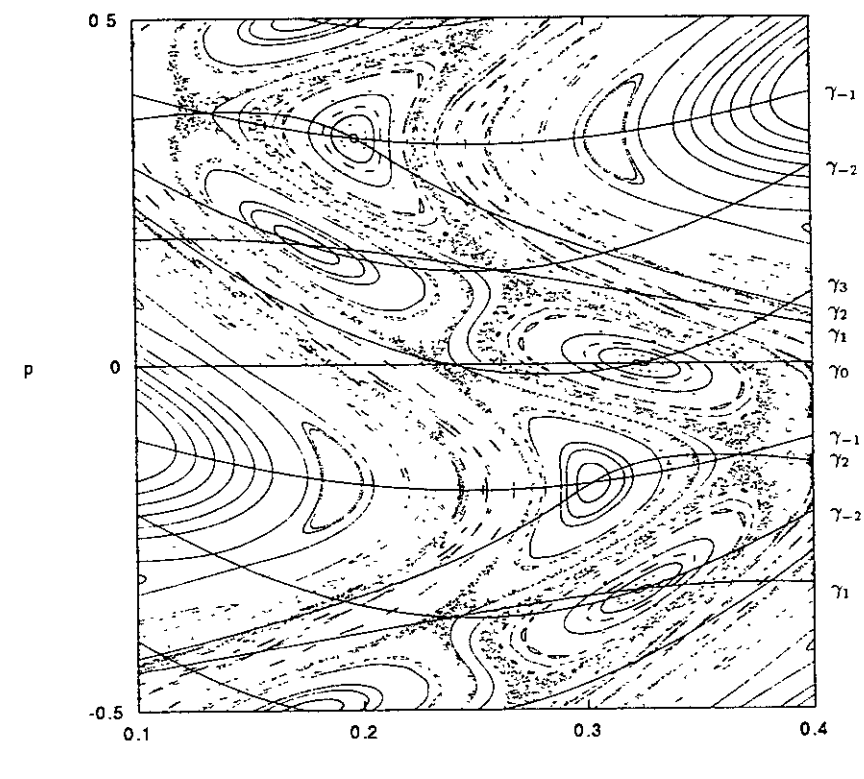
0 5
0
-0.5
p
0.1
0.2
0.3
0.4
q
γ−1
γ−2
γ3
γ2
γ1
γ0
γ−1
γ2
γ−2
γ1

Fig 6

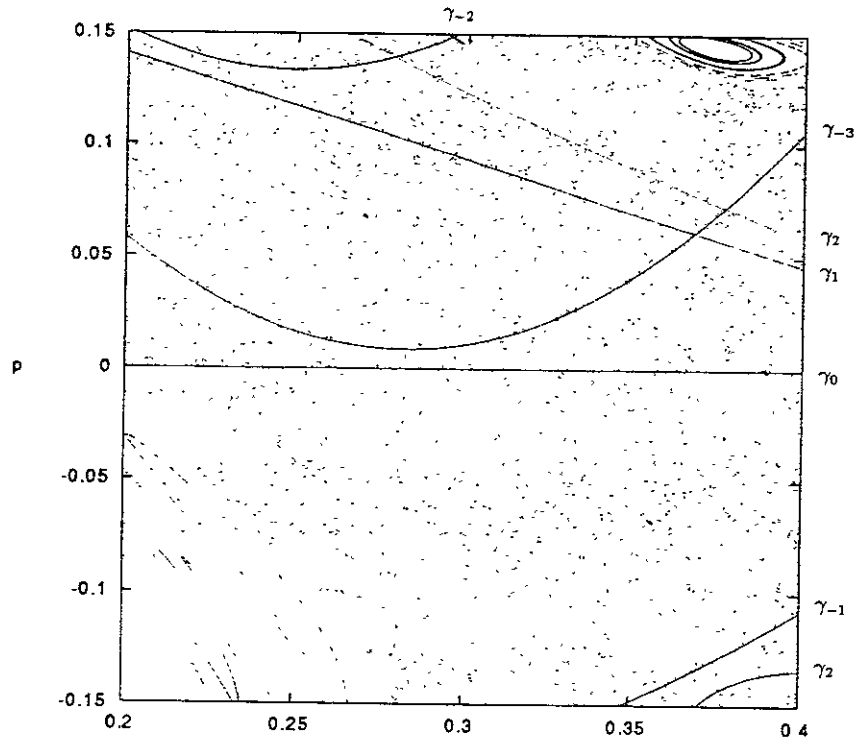
γ_{-2}
0.15
0.1
0.05
0
-0.05
-0.1
-0.15
p
γ_{-3}
γ_2
γ_1
γ_0
γ_{-1}
γ_2
0.2
0.25
0.3
0.35
0 4
q

Fig. 7

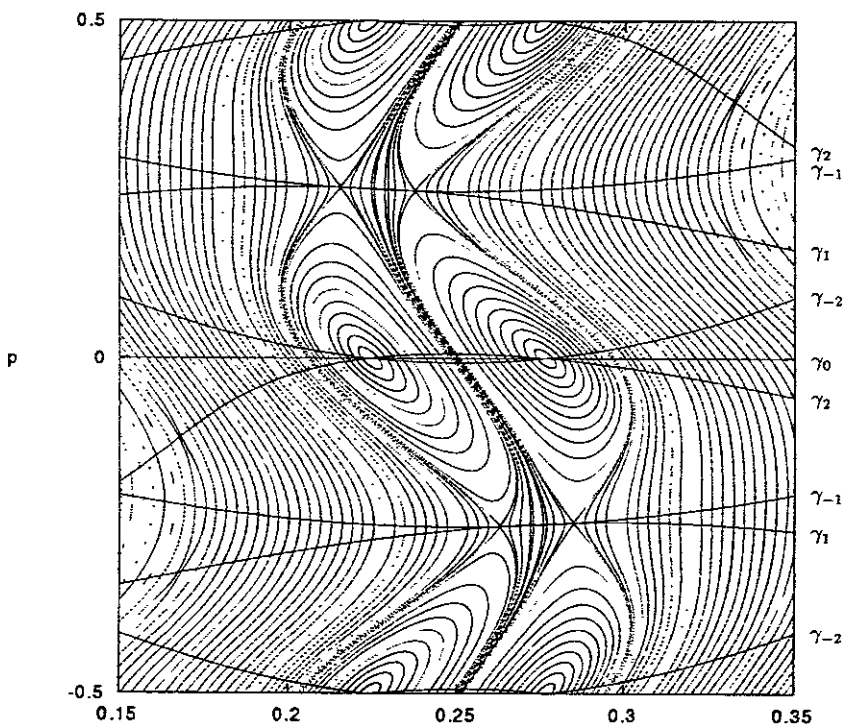
0.5
0
-0.5
p
γ_2
γ_{-1}
γ_1
γ_{-2}
γ_0
γ_2
γ_{-1}
γ_1
γ_{-2}
0.15
0.2
0.25
0.3
0.35
q

Fig. 8

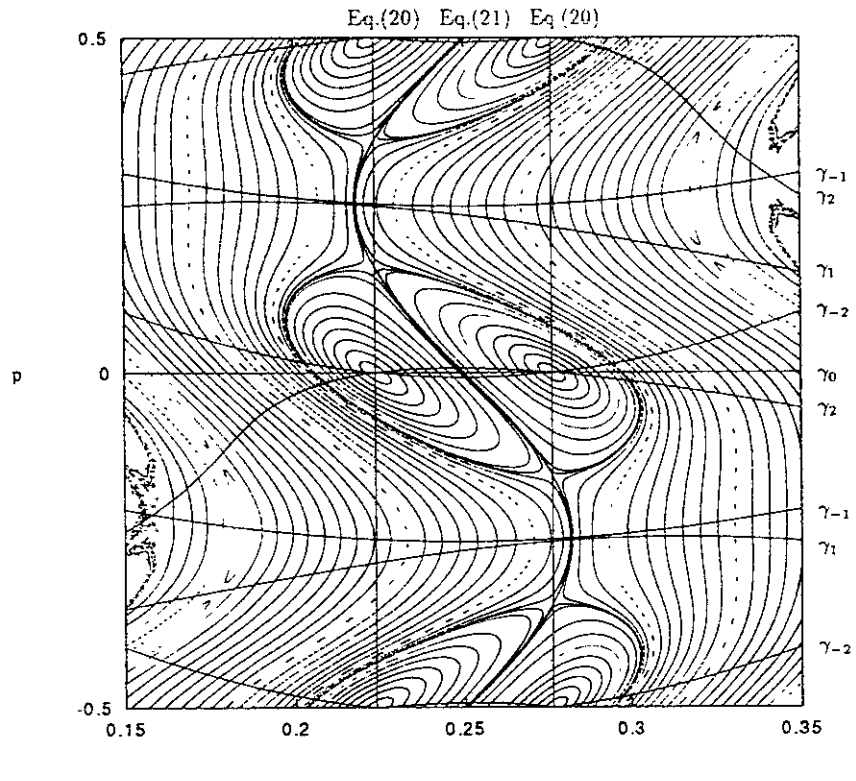
Eq.(20) Eq.(21) Eq.(20)
0.5
0
-0.5
p
0.15
0.2
0.25
0.3
0.35
q
γ-1
γ2
γ1
γ-2
γ0
γ2
γ-1
γ1
γ-2

Fig. 9

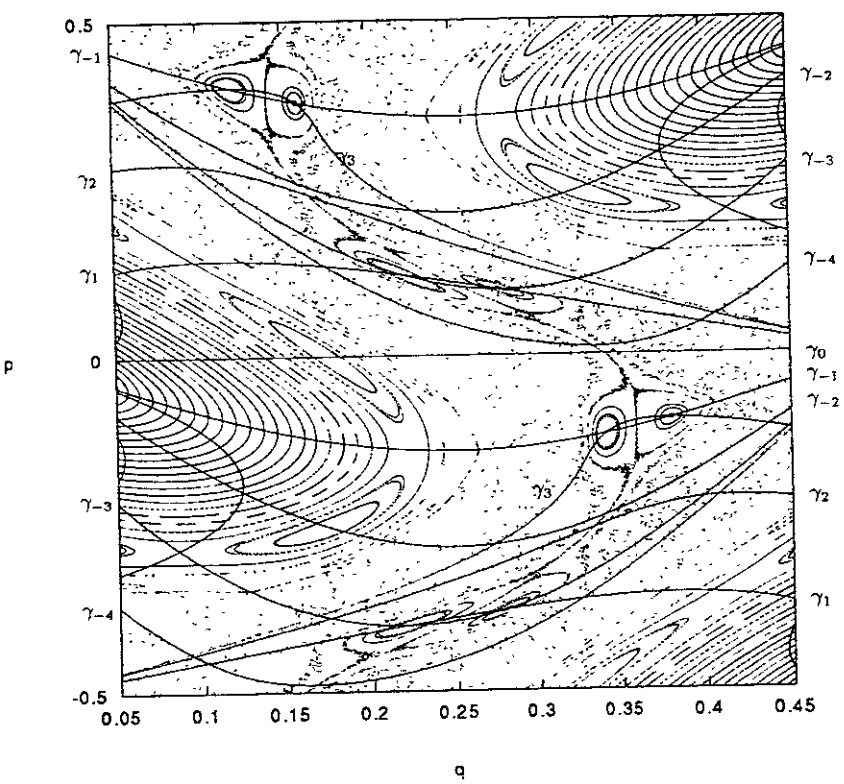
0.5
γ-1
γ2
γ1
0
p
γ-3
γ-4
-0.5
0.05
0.1
0.15
0.2
0.25
0.3
0.35
0.4
0.45
q
γ-2
γ-3
γ-4
γ0
γ-1
γ-2
γ2
γ1
γ3
γ3

Fig. 10

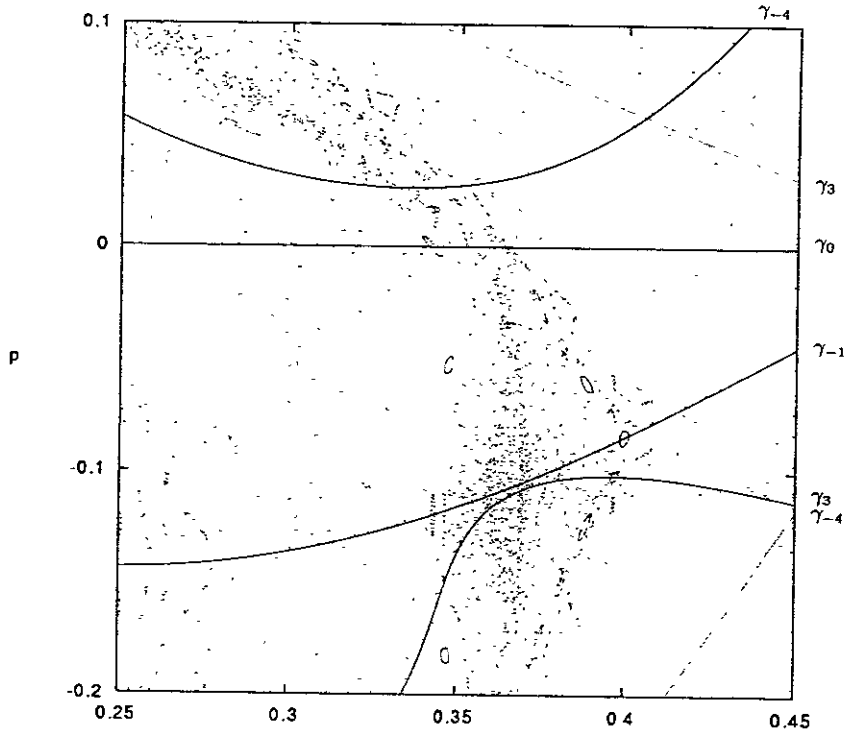

Fig 11

A	L	Period	Step
6.37	0.1	1	1
3.185	0.4	2	1
2.3	0.9	3	1
1.8	1.15	4	1
1.5	1.0	5	1
1.305	0.98	6	1
1.3	1.105	20	3
1.3	1.075	13	2
1.2	1.05	15	2
1.17	0.93	7	1
1.1	1.015	9	1
1.1	0.954	8	1
1.07	1.02114	10	1
1.06	0.988	19	2
1.0	0.9575	11	1
0.904	0.889	14	1
0.9	0.86	12	1
0.85	0.8439	17	1
0.84	0.8305	16	1
0.8	0.79464	18	1

Recent Issues of NIFS Series

NIFS-417 T. Yabe, H. Daido,T. Aoki, E. Matsunaga and K. Arisawa,
Anomalous Crater Formation in Pulsed-Laser-Illuminated Aluminum Slab and Debris Distribution; May 1996

NIFS-418 J. Uramoto,
Extraction of K^- Mesonlike Particles from a D_2 Gas Discharge Plasma in Magnetic Field; May 1996

NIFS-419 J. Xu, K. Toi, H. Kuramoto, A. Nishizawa, J. Fujita, A. Ejiri, K. Narihara, T. Seki, H. Sakakita, K. Kawahata, K. Ida, K. Adachi, R. Akiyama, Y. Hamada, S. Hirokura, Y. Kawasumi, M. Kojima, I. Nomura, S. Ohdachi, K.N. Sato
Measurement of Internal Magnetic Field with Motional Stark Polarimetry in Current Ramp-Up Experiments of JIPP T-IIU; June 1996

NIFS-420 Y.N. Nejoh,
Arbitrary Amplitude Ion-acoustic Waves in a Relativistic Electron-beam Plasma System; July 1996

NIFS-421 K. Kondo, K. Ida, C. Christou, V.Yu.Sergeev, K.V.Khlopenkov, S.Sudo, F. Sano, H. Zushi, T. Mizuuchi, S. Besshou, H. Okada, K. Nagasaki, K. Sakamoto, Y. Kurimoto, H. Funaba, T. Hamada, T. Kinoshita, S. Kado, Y. Kanda, T. Okamoto, M. Wakatani and T. Obiki,
Behavior of Pellet Injected Li Ions into Heliotron E Plasmas; July 1996

NIFS-422 Y. Kondoh, M. Yamaguchi and K. Yokozuka,
Simulations of Toroidal Current Drive without External Magnetic Helicity Injection; July 1996

NIFS-423 Joong-San Koog,
Development of an Imaging VUV Monochromator in Normal Incidence Region; July 1996

NIFS-424 K. Orito,
A New Technique Based on the Transformation of Variables for Nonlinear Drift and Rossby Vortices; July 1996

NIFS-425 A. Fujisawa, H. Iguchi, S. Lee, T.P. Crowley, Y. Hamada, H. Sanuki, K. Itoh, S. Kubo, H. Idei, T. Minami, K. Tanaka, K. Ida, S. Nishimura, S. Hidekuma, M. Kojima, C. Takahashi, S. Okamura and K. Matsuoka,
Direct Observation of Potential Profiles with a 200keV Heavy Ion Beam Probe and Evaluation of Loss Cone Structure in Toroidal Helical Plasmas on the Compact Helical System; July 1996

NIFS-426 H. Kitauchi, K. Araki and S. Kida,
Flow Structure of Thermal Convection in a Rotating Spherical Shell; July

1996

NIFS-427 S. Kida and S. Goto,
Lagrangian Direct-interaction Approximation for Homogeneous Isotropic Turbulence; July 1996

NIFS-428 V.Yu. Sergeev, K.V. Khlopenkov, B.V. Kuteev, S. Sudo, K. Kondo, F. Sano, H. Zushi, H. Okada, S. Besshou, T. Mizuuchi, K. Nagasaki, Y. Kurimoto and T. Obiki,
Recent Experiments on Li Pellet Injection into Heliotron E; Aug. 1996

NIFS-429 N. Noda, V. Philipps and R. Neu,
A Review of Recent Experiments on W and High Z Materials as Plasma-Facing Components in Magnetic Fusion Devices; Aug. 1996

NIFS-430 R.L. Tobler, A. Nishimura and J. Yamamoto,
Design-Relevant Mechanical Properties of 316-Type Stainless Steels for Superconducting Magnets; Aug. 1996

NIFS-431 K. Tsuzuki, M. Natsir, N. Inoue, A. Sagara, N. Noda, O. Motojima, T. Mochizuki, T. Hino and T. Yamashina,
Hydrogen Absorption Behavior into Boron Films by Glow Discharges in Hydrogen and Helium; Aug. 1996

NIFS-432 T.-H. Watanabe, T. Sato and T. Hayashi,
Magnetohydrodynamic Simulation on Co- and Counter-helicity Merging of Spheromaks and Driven Magnetic Reconnection; Aug. 1996

NIFS-433 R. Horiuchi and T. Sato,
Particle Simulation Study of Collisionless Driven Reconnection in a Sheared Magnetic Field; Aug. 1996

NIFS-434 Y. Suzuki, K. Kusano and K. Nishikawa,
Three-Dimensional Simulation Study of the Magnetohydrodynamic Relaxation Process in the Solar Corona. II.; Aug. 1996

NIFS-435 H. Sugama and W. Horton,
Transport Processes and Entropy Production in Toroidally Rotating Plasmas with Electrostatic Turbulence; Aug. 1996

NIFS-436 T. Kato, E. Rachlew-Källne, P. Hörling and K.-D Zastrow,
Observations and Modelling of Line Intensity Ratios of OV Multiplet Lines for 2s3s 3S1 - 2s3p 3Pj; Aug. 1996

NIFS-437 T. Morisaki, A. Komori, R. Akiyama, H. Idei, H. Iguchi, N. Inoue, Y. Kawai, S. Kubo, S. Masuzaki, K. Matsuoka, T. Minami, S. Morita, N. Noda, N. Ohyabu, S. Okamura, M. Osakabe, H. Suzuki, K. Tanaka, C. Takahashi, H. Yamada, I. Yamada and O. Motojima,
Experimental Study of Edge Plasma Structure in Various Discharges on

Compact Helical System; Aug. 1996

NIFS-438 A. Komori, N. Ohyabu, S. Masuzaki, T. Morisaki, H. Suzuki, C. Takahashi, S. Sakakibara, K. Watanabe, T. Watanabe, T. Minami, S. Morita, K. Tanaka, S. Ohdachi, S. Kubo, N. Inoue, H. Yamada, K. Nishimura, S. Okamura, K. Matsuoka, O. Motojima, M. Fujiwara, A. Iiyoshi, C. C. Klepper, J.F. Lyon, A.C. England, D.E. Greenwood, D.K. Lee, D.R. Overbey, J.A. Rome, D.E. Schechter and C.T. Wilson,
Edge Plasma Control by a Local Island Divertor in the Compact Helical System; Sep. 1996 (IAEA-CN-64/C1-2)

NIFS-439 K. Ida, K. Kondo, K. Nagaski T. Hamada, H. Zushi, S. Hidekuma, F. Sano, T. Mizuuchi, H. Okada, S. Besshou, H. Funaba, Y. Kurimoto, K. Watanabe and T. Obiki,
Dynamics of Ion Temperature in Heliotron-E; Sep. 1996 (IAEA-CN-64/CP-5)

NIFS-440 S. Morita, H. Idei, H. Iguchi, S. Kubo, K. Matsuoka, T. Minami, S. Okamura, T. Ozaki, K. Tanaka, K. Toi, R. Akiyama, A. Ejiri, A. Fujisawa, M. Fujiwara, M. Goto, K. Ida, N. Inoue, A. Komori, R. Kumazawa, S. Masuzaki, T. Morisaki, S. Muto, K. Narihara, K. Nishimura, I. Nomura, S. Ohdachi, M.. Osakabe, A. Sagara, Y. Shirai, H. Suzuki, C. Takahashi, K. Tsumori, T. Watari, H. Yamada and I. Yamada,
A Study on Density Profile and Density Limit of NBI Plasmas in CHS; Sep. 1996 (IAEA-CN-64/CP-3)

NIFS-441 O. Kaneko, Y. Takeiri, K. Tsumori, Y. Oka, M. Osakabe, R. Akiyama, T. Kawamoto, E. Asano and T. Kuroda,
Development of Negative-Ion-Based Neutral Beam Injector for the Large Helical Device; Sep. 1996 (IAEA-CN-64/GP-9)

NIFS-442 K. Toi, K.N. Sato, Y. Hamada, S. Ohdachi, H. Sakakita, A. Nishizawa, A. Ejiri, K. Narihara, H. Kuramoto, Y. Kawasumi, S. Kubo, T. Seki, K. Kitachi, J. Xu, K. Ida, K. Kawahata, I. Nomura, K. Adachi, R. Akiyama, A. Fujisawa, J. Fujita, N. Hiraki, S. Hidekuma, S. Hirokura, H. Idei, T. Ido, H. Iguchi, K. Iwasaki, M. Isobe, O. Kaneko, Y. Kano, M. Kojima, J. Koog, R. Kumazawa, T. Kuroda, J. Li, R. Liang, T. Minami, S. Morita, K. Ohkubo, Y. Oka, S. Okajima, M. Osakabe, Y. Sakawa, M. Sasao, K. Sato, T. Shimpo, T. Shoji, H. Sugai, T. Watari, I. Yamada and K. Yamauti,
Studies of Perturbative Plasma Transport, Ice Pellet Ablation and Sawtooth Phenomena in the JIPP T-IIU Tokamak; Sep. 1996 (IAEA-CN-64/A6-5)

NIFS-443 Y. Todo, T. Sato and The Complexity Simulation Group,
Vlasov-MHD and Particle-MHD Simulations of the Toroidal Alfvén Eigenmode; Sep. 1996 (IAEA-CN-64/D2-3)

NIFS-444 A. Fujisawa, S. Kubo, H. Iguchi, H. Idei, T. Minami, H. Sanuki, K. Itoh, S. Okamura, K. Matsuoka, K. Tanaka, S. Lee, M. Kojima, T.P. Crowley, Y. Hamada, M. Iwase, H. Nagasaki, H. Suzuki, N. Inoue, R. Akiyama, M. Osakabe, S. Morita,

C. Takahashi, S. Muto, A. Ejiri, K. Ida, S. Nishimura, K. Narihara, I. Yamada, K. Toi, S. Ohdachi, T. Ozaki, A. Komori, K. Nishimura, S. Hidekuma, K. Ohkubo, D.A. Rasmussen, J.B. Wilgen, M. Murakami, T. Watari and M. Fujiwara,
An Experimental Study of Plasma Confinement and Heating Efficiency through the Potential Profile Measurements with a Heavy Ion Beam Probe in the Compact Helical System; Sep. 1996 (IAEA-CN-64/C1-5)

NIFS-445 O. Motojima, N. Yanagi, S. Imagawa, K. Takahata, S. Yamada, A. Iwamoto, H. Chikaraishi, S. Kitagawa, R. Maekawa, S. Masuzaki, T. Mito, T. Morisaki, A. Nishimura, S. Sakakibara, S. Satoh, T. Satow, H. Tamura, S. Tanahashi, K. Watanabe, S. Yamaguchi, J. Yamamoto, M.Fujiwara and A. Iiyoshi,
Superconducting Magnet Design and Construction of LHD; Sep. 1996 (IAEA-CN-64/G2-4)

NIFS-446 S. Murakami, N. Nakajima, S. Okamura, M. Okamoto and U. Gasparino,
Orbit Effects of Energetic Particles on the Reachable β–Value and the Radial Electric Field in NBI and ECR Heated Heliotron Plasmas; Sep. 1996 (IAEA-CN-64/CP -6) Sep. 1996

NIFS-447 K. Yamazaki, A. Sagara, O. Motojima, M. Fujiwara, T. Amano, H. Chikaraishi, S. Imagawa, T. Muroga, N. Noda, N. Ohyabu, T. Satow, J.F. Wang, K.Y. Watanabe, J. Yamamoto , H. Yamanishi, A. Kohyama, H. Matsui, O. Mitarai, T. Noda, A.A. Shishkin, S. Tanaka and T. Terai
Design Assessment of Heliotron Reactor; Sep. 1996 (IAEA-CN-64/G1-5)

NIFS-448 M. Ozaki, T. Sato and the Complexity Simulation Group,
Interactions of Convecting Magnetic Loops and Arcades; Sep. 1996

NIFS-449 T. Aoki,
Interpolated Differential Operator (IDO) Scheme for Solving Partial Differential Equations; Sep. 1996

NIFS-450 D. Biskamp and T. Sato,
Partial Reconnection in the Sawtooth Collapse; Sep. 1996

NIFS-451 J. Li, X. Gong, L. Luo, F.X. Yin, N. Noda, B. Wan, W. Xu, X. Gao, F. Yin, J.G. Jiang, Z. Wu., J.Y. Zhao. M. Wu, S. Liu and Y. Han,
Effects of High Z Probe on Plasma Behavior in HT-6M Tokamak; Sep. 1996

NIFS-452 N. Nakajima, K. Ichiguchi, M. Okamoto and R.L. Dewar,
Ballooning Modes in Heliotrons/Torsatrons; Sep. 1996 (IAEA-CN-64/D3-6)

NIFS-453 A. Iiyoshi,
Overview of Helical Systems; Sep. 1996 (IAEA-CN-64/O1-7)

NIFS-454 S. Saito, Y. Nomura, K. Hirose and Y.H. Ichikawa,
Separatrix Reconnection and Periodic Orbit Annihilation in the Harper Map; Oct. 1996